

Chapter 1

Non-equilibrium Green Functions and the Transport Problem

1.1 Setting up the transport problem

The new paradigm imposed by nanotechnology is the need for a complete quantum mechanical description of electronic transport. At the atomic level a classical description of physical systems gives way to quantum mechanics - and in some cases, special relativity. As we have already mentioned, decreasing the sizes of electronic devices presents tantalising perspectives, however the road ahead might be quite bumpy. Firstly, new fabrication methods need to be devised as we are reaching the limits in size resolution for current ones. Secondly, when modelling atomic scale circuits, one must introduce a treatment in terms of wave functions and transmission probabilities, an aspect usually ignored in conventional electronic engineering.

The typical system one wishes to study in atomic scale transport problems is presented in figure (1.1a). It is a two-probe device consisting of two charge reservoirs bridged by a nanoscale object, namely a molecule or a surface. In a real world scenario this component would be integrated, in a variety of ways, with a number of similar components for logic and/or data storage applications. There are a number of questions that need to be answered before we can attempt to mass produce these nanoscale devices. In fact, we still understand very little about the electronic transport properties of a single atomic size device.

A clearer understanding is imperative if we want to use such systems for technological applications. Therefore throughout this work, we will focus on a single device, a task difficult enough as it is.

Figure (1.1) pictures the same problem from three different perspectives. From a thermodynamic point of view the system comprises two bulk leads and a central region. The latter includes the actual device and, for reasons that will be clear later,

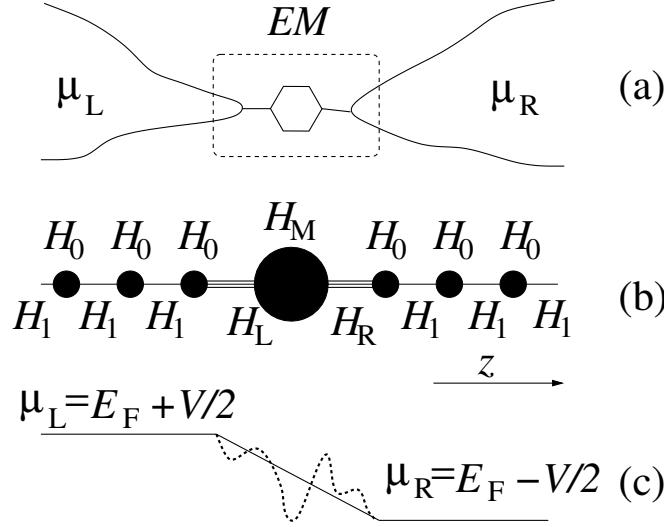


Figure 1.1: Schematic representation of the transport problem from three different perspectives: (a) thermodynamical, (b) quantum mechanical and (c) electrostatical.

part of the leads. Therefore we call such central region an “extended molecule” (EM).¹ The two current/voltage leads are kept at two different chemical potentials respectively μ_L and μ_R and are able to exchange electrons with the EM. Note that when the applied bias is zero ($\mu_L = \mu_R$), this system of interacting electrons is in thermodynamic equilibrium and may be regarded as a grand canonical ensemble. When the bias is applied however $\mu_L \neq \mu_R$ and the current will flow. The prescription for establishing the steady state is that of adiabatically switching on the coupling between the leads and the EM [63, 89, 90].

One important aspect that is missing from figure (1.1a) is the battery. A battery is connected to the ends of the charge reservoirs and a potential difference is applied. Effectively this bias is what keeps the two chemical potentials μ_L and μ_R different. The effect will be of charge flowing across the device, from one reservoir into another to try to counter-balance the effect of the external bias: the current.

At the Hamiltonian level the system under investigation is described by an infinite hermitian matrix \mathcal{H} .² We assume that our system has a rather regular structure, in particular the electrodes. This is by no means the general case but an assumption.

¹Hereafter we refer to “molecule” as any system comprising a finite number of atoms, e. g. a segment of a carbon nanotube. This includes also extended surfaces, finite along the transport direction, such as in tunnelling junctions.

²Throughout this work we use calligraphic symbols to denote infinite matrices and capitalised characters for finite ones

tion that makes the problem solvable. First notice that the two semi-infinite current/voltage probes are defect-free crystalline metals. These have a regular periodic structure and a unit cell along which the direction of the transport can be defined. The second assumption is that the transport problem will be formulated in terms of a linear combination of atomic orbitals (LCAO). Despite the rather general choice of basis it is clear that the total Hamiltonian for the system is going to be rather sparse. Given the sparsity of the total Hamiltonian it is convenient to introduce the concept of principal layer (PL). A principal layer is the smallest cell that repeats periodically in the direction of transport. It is constructed in such a way to interact only with the nearest neighbour PLs. This means that *all* the matrix elements between atoms belonging to two non-adjacent PLs vanish.

For example take a linear chain of hydrogen atoms described by a nearest neighbour tight-binding model then one atom forms the PL. However if nearest and next nearest neighbour elements are included then the PL will contain two atoms, etc (for examples see section 1.6.2). A more general case would be that of a PL formed by N_{species} types of atoms (atomic species) with N_{atoms}^i atoms of species i and each species comprising of N_{orbitals}^i orbitals (basis functions).

We then define H_0 as the $N \times N$ matrix describing all interactions within a PL, where

$$N = \sum_i^{N_{\text{species}}} N_{\text{atoms}}^i \times N_{\text{orbitals}}^i, \quad (1.1)$$

is the total number of degrees of freedom (total number of basis functions) in the PL. Similarly H_1 is the $N \times N$ matrix describing the interaction between two PLs. Finally H_M is the $M \times M$ matrix describing the extended molecule and H_{LM} (H_{RM}) is the $N \times M$ matrix containing the interaction between the last PL of the left-hand side (right-hand side) lead and the extended molecule. The final form of \mathcal{H} is

$$\mathcal{H} = \begin{pmatrix} \cdot & \cdot & \cdot & \cdot & \cdot & \cdot & \cdot & \cdot & \cdot & \cdot & \cdot \\ \cdot & 0 & H_{-1} & H_0 & H_1 & 0 & \cdot & \cdot & \cdot & \cdot & \cdot \\ \cdot & \cdot & 0 & H_{-1} & H_0 & H_{LM} & 0 & \cdot & \cdot & \cdot & \cdot \\ \cdot & \cdot & \cdot & 0 & H_{ML} & H_M & H_{MR} & 0 & \cdot & \cdot & \cdot \\ \cdot & \cdot & \cdot & \cdot & 0 & H_{RM} & H_0 & H_1 & 0 & \cdot & \cdot \\ \cdot & \cdot & \cdot & \cdot & \cdot & 0 & H_{-1} & H_0 & H_1 & 0 & \cdot \\ \cdot & \cdot & \cdot & \cdot & \cdot & \cdot & \cdot & \cdot & \cdot & \cdot & \cdot \end{pmatrix}. \quad (1.2)$$

For a system which preserves time-reversal symmetry $H_{-1} = H_1^\dagger$, $H_{ML} = H_{LM}^\dagger$ and $H_{MR} = H_{RM}^\dagger$. In this form \mathcal{H} has the same structure as the Hamiltonian of a one-dimensional system as shown in figure 1.1b. However this is not the most general

situation and does not apply if a magnetic field is present for example. Also note that \mathcal{H} is tridiagonal.

For a non-orthogonal basis set the overlap matrix \mathcal{S} has exactly the same structure of \mathcal{H} . Therefore we adopt the notation S_0 , S_1 , S_{LM} , S_{RM} and S_M for the various blocks of \mathcal{S} , in complete analogy with their Hamiltonian counterparts. Here the principal layer, defined for \mathcal{H} is used for both the \mathcal{S} and the \mathcal{H} matrix, even though the range of \mathcal{S} can be considerably shorter than that of \mathcal{H} .

Let us now discuss the electrostatics of the problem (figure 1.1c). The main consideration here is that the current/voltage probes are made from good metals and therefore preserve local charge neutrality. For this reason the effect of an external bias voltage on the leads will produce a rigid shift of the whole spectrum, i.e. of all the on-site energies. In contrast a non-trivial potential profile will develop over the extended molecule, which needs to be calculated self-consistently. Importantly the resulting self-consistent electrostatic potential must match that of the leads at the boundaries of the EM. If this does not happen, the potential profile will develop a discontinuity with the generation of spurious scattering. Therefore, in order to achieve a good match of the electrostatic potential, several layers of the leads are usually included in the extended molecule. Their number ultimately depends upon the screening length of the leads, but in most situations a few (between two and four) atomic planes are sufficient.

Moreover, even in the case of extremely short screening length, it is good practice to include a few planes of the leads in the extended molecule because the electrodes generally have reconstructed surfaces, which might undergo additional geometrical reconstructions when bonding to a nanoscale device (e.g. molecules attached to metallic surfaces through corrosive chemical groups).

In order to find the electron's wavefunction and determine the full quantum mechanical properties of the problem one, in principle, needs to diagonalise \mathcal{H} . However, the Hamiltonian is clearly neither finite nor translationally invariant (the terms H_{LM} , H_{ML} , H_{MR} , H_{RM} , H_M break translational symmetry). Hence, Bloch's theorem cannot be applied for the entire system and we need to diagonalise an infinite matrix; clearly an impossible task.

This issue must be addressed in a different way. A possible way is to assume that states deep inside the electrodes are associated to Bloch states of the infinite system. These states are scattered by the potential created by the central EM. One can then use a Green function [61, 63] or a wavefunction approach [91, 92] to calculate the ground state electronic properties (including the wavefunction) of an open system.

The resulting wavefunction can be considered as a combination of Bloch states for the region inside the electrodes and localised atomic-like states for the region in and around the EM.

Even if one is able to calculate the Hamiltonian \mathcal{H} (and the electron wavefunction) the problem of transport still needs to be addressed. We do so by looking at two different limits. Firstly the limit of infinitesimally small bias: the linear regime. In this limit, we can formulate a quantum mechanical description of our problem lying at or close to equilibrium conditions. We assume that under an external applied bias the Hamiltonian $\mathcal{H}(V)$ does not significantly change from that of the ground-state $\mathcal{H}(V=0)$. This approach will be presented in section 1.2 where we show using the Landauer-Büttiker formalism [84] that the transport properties, most notably the conductance can be associated with the transmission probabilities of the scattered part of the electronic wavefunction.

Secondly, we will present, in section (1.3), a very simple model of transport across a single energy level in order to understand changes to the system's Hamiltonian under bias - an effect we neglected in the previous situation case. The total current at steady state can be associated to the rate of transfer of electrons across the EM. These two simple cases will lead to a deeper understanding of the transport problem. We will then join these two concepts into a more general framework which we present in section (1.4).

1.2 The Landauer formalism: equilibrium transport

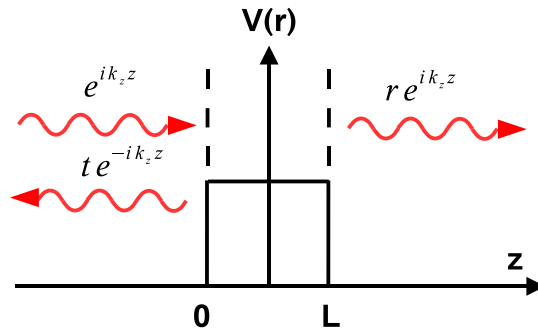


Figure 1.2: Schematic representation of incoming and outgoing wavefunctions scattered by a potential $V(r)$

The Landauer-Büttiker formalism [84] associates the conductance of a device with

the quantum mechanical transmission probabilities of the one electron wave function as it approaches an arbitrary scattering potential [61]. There are two underlying assumptions in this formulation namely: the electrodes must be both in thermal equilibrium devoid of correlation effects.

The problem can be formulated in terms of incoming, $|\Phi_{in}\rangle$ and outgoing, $|\Phi_{out}\rangle$ electron wavefunctions propagating along a one dimensional wire (scattering channel) and scattered by a potential connecting the two leads. Due to the periodic nature of the wire, these wavefunctions have the form of Bloch waves and in absence of a scattering potential, each one contributes with $2e^2/h = G_0$ to the total conductance [84]. We then define the scattering channel as the asymptotic part of the wavefunction deep inside the leads. If the system is multi-dimensional (quasi- 1D, 2D or 3D), several possible Bloch waves with the same energy can propagate through the leads (multi-channel problem). Once the i -th channel in the left hand-side reaches the scattering region it can be transmitted to any channel into the right hand-side lead or back scattered into any channels of the left hand-side lead.

Figure (1.2) provides a simple example of the transport problem formulated in terms of in-scattering and out-scattering channels: free electrons with energy E are injected from the left and are scattered by a step potential

$$V(z) = \begin{cases} V & , \quad z < L \\ 0 & , \quad \text{elsewhere} \end{cases} . \quad (1.3)$$

As we can see, an incoming electron with wave-vector k_z is partially backscattered with wave-vector $-k_z$ and partially transmitted. The total wavefunction for this problem reads

$$|\Phi_{Total}\rangle = |\Phi_{in}\rangle + |\Phi_{0L}\rangle + |\Phi_{out}\rangle , \quad (1.4)$$

with

$$\langle z|\Phi_{Total}\rangle = \begin{cases} \langle z|\Phi_{in}\rangle = e^{ik_z z} + r e^{-ik_z z} & 0 \leq z \\ \langle z|\Phi_{0L}\rangle = A e^{\kappa_z z} + B e^{-\kappa_z z} & 0 \leq z \leq L \\ \langle z|\Phi_{out}\rangle = t e^{ik_z z} & z > L \end{cases} . \quad (1.5)$$

where the wave-vector k_z is given by

$$k_z = \frac{\sqrt{2mE}}{\hbar} , \quad (1.6)$$

whereas

$$\kappa_z = \frac{\sqrt{2m(V-E)}}{\hbar} , \quad (1.7)$$

can be real (evanescent) or imaginary (propagating) depending on whether $V > E$ or $V < E$ respectively. The coefficients A , B , t and r are determined by imposing

the continuity of the total wavefunction and its derivative at the boundaries of the step potential. Finally

$$|r|^2 + |t|^2 = 1, \quad (1.8)$$

i.e., the flux is conserved.

Alternatively the scattering process can be described in terms of the scattering matrix, S , which relates the wavefunction of the incoming and outgoing electrons with respect to the step potential *i. e.*, channels entering ($|\Phi_{in}\rangle$) or leaving ($|\Phi_{out}\rangle$) the region $0 \leq x \leq L$:

$$|\Phi_{in}\rangle = S|\Phi_{out}\rangle \quad (1.9)$$

where

$$S = \begin{pmatrix} r & t' \\ t & r' \end{pmatrix}, \quad (1.10)$$

and t and r are the transmission and reflexion coefficients respectively for incoming waves from the left whereas t' and r' are the counter parts for incoming waves from the right. In the more general multi-channel problem r , t , r' and t' are matrices.

Following Landauer [84], we can define the total conductance as ³

$$\Gamma = \frac{e^2}{h} \sum_{\sigma} \sum'_{ij} T_{ij}^{\sigma} = \frac{e^2}{h} \sum_{\sigma} Tr [t_{\sigma} t_{\sigma}^{\dagger}] = \frac{G_0}{2} \sum_{\sigma} Tr [t_{\sigma} t_{\sigma}^{\dagger}] \quad (1.11)$$

where \sum'_{ij} indicates that the sum is performed over all channels at the Fermi energy (E_F) (the open channels) and we have introduced the spin index σ ($\sigma = \uparrow, \downarrow$). We can clearly see that the conductance is written in terms of the conductance quantum G_0 . Most importantly we note that the conductance has been directly associated with the coefficients of the out-scattered wavefunctions of our simple problem. Hence the energy-dependent transmission probability

$$T^{\sigma}(E) = Tr [t_{\sigma}(E) t_{\sigma}^{\dagger}(E)].^4 \quad (1.12)$$

1.3 A simple model for transport under bias

Before laying the theoretical framework which is the main subject of this dissertation we will take some time to introduce a simple model for electronic transport under bias.

³In the case presented here we are already considering the more general situation of a non spin-degenerate system, so the Hilbert space spans over the spin degrees of freedom σ as well. For that reason the universal quantum of conductance, G_0 is divided by two.

⁴In our simple problem this reduces to $T(E) = |t(E)|^2$.

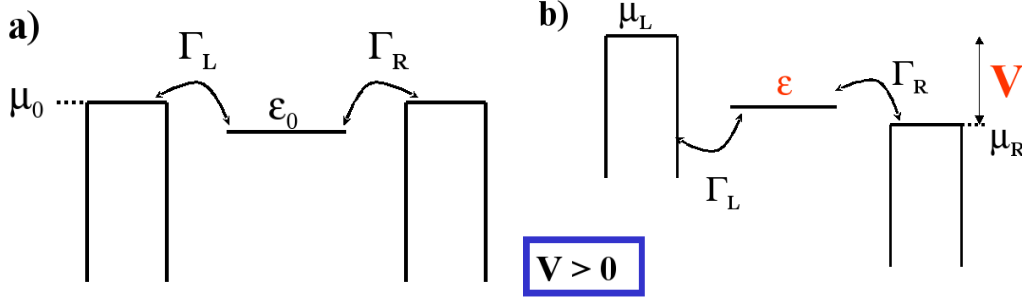


Figure 1.3: Schematic picture of a single energy level - representing a molecule - sandwiched between two jellium reservoirs each with a chemical potential μ_0 . The coupling between the molecular state and the leads is given by Γ_L and Γ_R .

We model our system by sandwiching a molecule between two charge reservoirs. We represent a molecule as a single energy level ϵ_0 . The electrodes are modelled as jellium (constant density of states) with chemical potential set at μ_0 (in the case of thermodynamic equilibrium the chemical potential μ_0 coincides with the Fermi level E_F). When the molecule is attached to the electrodes, the strength of the coupling to the left- and right-hand-side lead is given by Γ_L and Γ_R respectively (see figure (1.3)), *i. e.* the hopping probabilities are Γ_L/\hbar and Γ_R/\hbar . We can write an effective Hamiltonian for our system as the original on-site energy and include the effects of the coupling to the electrodes in terms of a imaginary part added to it

$$\epsilon' = \epsilon_0 + i\frac{\Gamma_L}{2} + i\frac{\Gamma_R}{2}. \quad (1.13)$$

In doing so we only need to focus on the molecule, assuming that the electrodes are not affected by changes due to the attached molecule.

While the density of states of the isolated molecule is a delta function

$$\delta(E - \epsilon_0) = \lim_{\eta \rightarrow 0^+} \frac{1}{\pi} \frac{\eta}{(E - \epsilon_0)^2 + \eta^2}, \quad (1.14)$$

that of the coupled system is given by a Lorentzian with broadening $\Gamma = \Gamma_L + \Gamma_R$,

$$DOS = \frac{1}{\pi} \Im \left(\frac{1}{E - \epsilon'} \right) = \frac{1}{2\pi} \frac{\Gamma_L + \Gamma_R}{(E - \epsilon)^2 + \left(\frac{\Gamma_L + \Gamma_R}{2}\right)^2}. \quad (1.15)$$

This broadening can be associated with the inverse lifetime of the electron on the molecule. In other words, the stronger the coupling the quicker the electron flows from (to) the electrode into (from) the molecule.

Initially, at $V=0$, the position of the chemical potential for both left and right

electrodes, μ_0 , is the same.⁵ When a bias is applied the chemical potential of the left electrode is shifted by $\frac{eV}{2}$ whereas that of the right hand-side lead changes by $-\frac{eV}{2}$. We assume, in this case, that the drop in the potential occurs at the two interfaces between the molecules and the electrodes. Therefore the position of the energy level remains unchanged. The new chemical potential of the left- and right-hand-side electrodes are now given by $\mu_L = \mu_0 + \frac{V}{2}$ and $\mu_R = \mu_0 - \frac{V}{2}$ respectively (see figure 1.3b)).

We now need to calculate the current under bias. Suppose the molecule is attached solely to the left electrode and $\epsilon < \mu_L$. Then electrons will flow from the left electrode into the molecule until the energy level is in thermodynamical equilibrium with the lead. The opposite happens if $\epsilon > \mu_L$, *i. e.*, electrons flow out of the molecule into the electrode until equilibrium is reached. At equilibrium, the occupation of the molecular state is driven by the chemical potential of the left electrode. It can be written as

$$N_L = 2f(\epsilon, \mu_L) \quad (1.16)$$

where $f(\epsilon, \mu_L)$ is the Fermi distribution at energy ϵ and chemical potential μ_L

$$f(\epsilon, \mu_L) = \frac{1}{e^{(\epsilon - \mu_L)/k_B T} + 1}, \quad (1.17)$$

k_B is the Boltzmann constant [93] and T is the temperature.

Analogously we can use the same arguments to calculate the occupation when the molecule is attached to the right-hand-side lead only

$$N_R = 2f(\epsilon, \mu_R). \quad (1.18)$$

Up to this point there is no current flowing through the system. The molecule is only connected to either the left- or the right-hand-side electrode and it is therefore in thermal equilibrium with either electrode. Once the molecule is connected to both left and right electrodes and bias is applied, we have three possible situations.

The first case is when $\epsilon_0 > \mu_L > \mu_R$, the molecular energy level is initially empty and above both chemical potentials. In this situation there are no electrons available for conduction and there will be no current (figure (1.4a)). The second case corresponds to $\epsilon_0 < \mu_R < \mu_L$. This time there are electrons which can flow from the

⁵For the sake of simplicity we are assuming that both left and right electrodes are made of the same material. We will show latter on in this chapter that one can use different electrodes with different chemical potentials. Once the molecule is attached to the left and to the right leads, there will be an equilibration of the chemical potential leading to a compensating electric field.

⁶The factor two in the equation indicates spin degeneracy. A non-spin-degenerate case could be derived analogously.

left electrode into the molecule, however there are no empty states available in the right lead. Therefore Pauli exclusion principle prevents current from flowing (figure (1.4b)). The third and most interesting scenario is when

$$\mu_R < \epsilon_0 < \mu_L, \quad (1.19)$$

i. e., the molecular state lies between the two chemical potentials. While electrons coming from the left electrode populate the molecule they can also leave for the right lead. Consequently current flows (see figure (1.4c)).

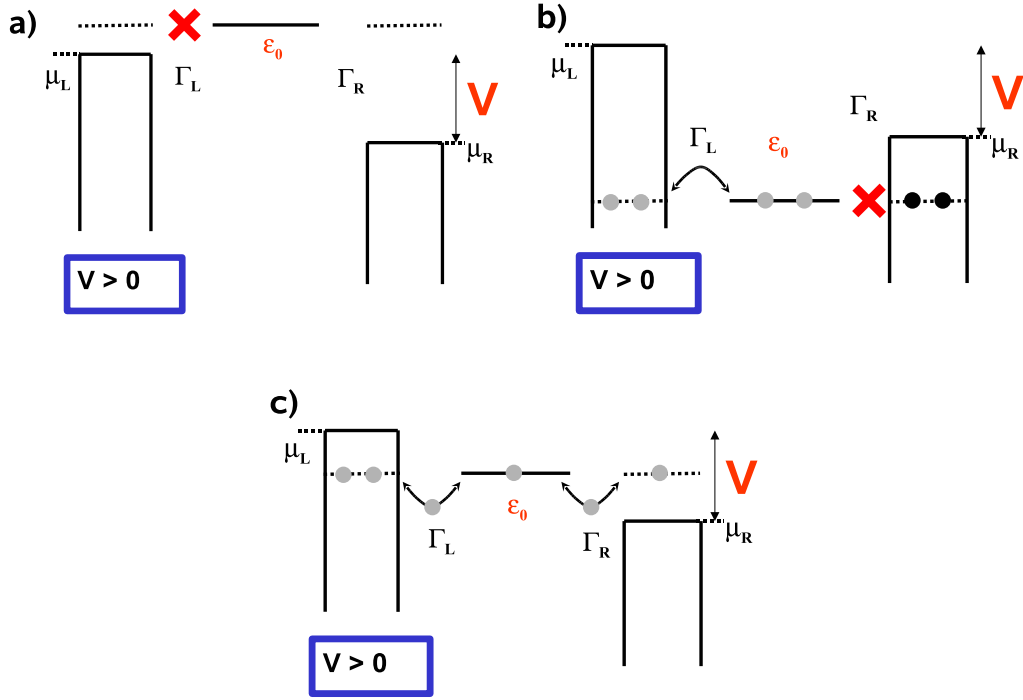


Figure 1.4: Diagram illustrating different positions of a molecular state with respect to the chemical potential of the semi-infinite electrodes. a) The energy level is higher than chemical potentials both in the right (μ_R) and in the left (μ_L) reservoirs \rightarrow no current. b) The energy level is lower than both chemical potentials \rightarrow no current. c) The energy level lies between μ_L and $\mu_R \rightarrow$ current.

Bearing in mind that the time-averaged non-equilibrium charge on the molecule corresponds to a value N in between N_L and N_R , then the current flowing from the left-hand-side lead to the molecule is simply

$$I_L = \frac{e\Gamma_L}{h} (N_L - N). \quad (1.20)$$

This equation shows that the current flowing into the molecule is proportionate to the number of excess electrons, *i. e.* to the charge difference $N_L - N$. Analogously,

the net current flowing from the molecule into the right electrode is

$$I_R = \frac{e\Gamma_R}{h} (N_R - N). \quad (1.21)$$

Initially, immediately after the coupling between the molecule and the leads has been switched on, the number of electrons flowing in and out of the molecule is going to vary as the molecule is reaching a steady state (a situation that will ultimately depend on the coupling to the left and right reservoirs). At steady state the number of electrons per unit time flowing from the left lead into the molecule and from the molecule into the right lead must be equal. By setting $I_L = I_R$ we obtain an expression for the occupation of the molecular level at the steady state

$$N = \frac{\Gamma_L f(\epsilon_0, \mu_L) + \Gamma_R f(\epsilon_0, \mu_R)}{\Gamma_L + \Gamma_R}. \quad (1.22)$$

Consequently, we can write an equation for the total current

$$I = \frac{2e}{h} \frac{\Gamma_L \Gamma_R}{\Gamma_L + \Gamma_R} (f(\epsilon_0, \mu_L) - f(\epsilon_0, \mu_R)). \quad (1.23)$$

In figure 1.5 we show the $I - V$ characteristics for different positions of the molecular state ϵ_0 . We can clearly see that, as long as the states lie outside the bias window, there is no current. However, for sufficiently high biases ϵ_0 will eventually be within the bias window and current will flow. In fact, the size of the gap in the current/voltage curve is given by $4|\mu_0 - \epsilon_0|$. Also note that the maximum current allowed through the junction is independent from the position of the energy level

$$I_{\max} = \frac{2e}{h} \frac{\Gamma_L \Gamma_R}{\Gamma_L + \Gamma_R} \quad (1.24)$$

1.3.1 Charging effects

The simple picture provided in the previous section shows how a balancing act between charge flowing in and out of the molecule will lead to electronic transport in conditions out of equilibrium. In order to make our model more realistic we can include changes to the Hamiltonian arising from changes in the occupation of the energy level. In simple terms, we would like to correct the on-site potential of the molecule to account for the electrostatic potential (classical) and possibly electron-electron (quantum) interactions.

As a simple approximation we assume that the energy level has the following form

$$\epsilon = \epsilon_0 + U_{\text{SCF}}, \quad (1.25)$$

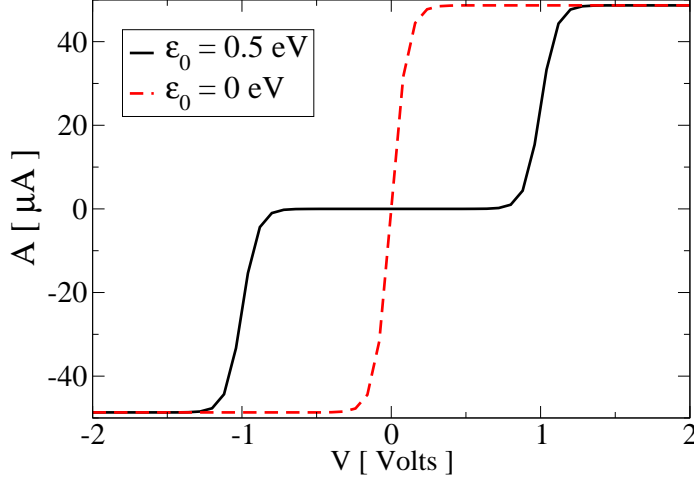


Figure 1.5: Current as a function of voltage for a molecule - represented by a single energy level - within two electrodes. In this case $\Gamma_L = \Gamma_R = 1$ eV and the molecular energy level is positioned either at the initial chemical potential μ_0 (dashed curve) or above it (solid line). The on-site energy is set to 0 and 0.5 eV respectively and $\mu_0 = 0$ eV. The case of $\epsilon_0 < \mu_0$ is the same as $\epsilon_0 > \mu_0$.

where the shift U_{SCF} is given by

$$U_{\text{SCF}} = U (N - 2f(\epsilon_0, \mu_0)). \quad (1.26)$$

We can clearly see that the term $f(\epsilon_0, \mu_0)$, the Fermi distribution for chemical potential μ_0 , corresponds to the initial occupation of the molecule at zero bias whereas N is the electronic population at a certain bias V (to be evaluated self-consistently). Therefore the term U_{SCF} indicates that the molecular state will shift - up or down - to account for changes in its population.

The non-equilibrium population N can be calculated in similar fashion to equation (1.22) if we replace ϵ_0 with ϵ . Now we need to calculate both quantities N and U_{SCF} self-consistently by iterating over equations (1.22), (1.25) and (1.26). This procedure must be repeated for each value of the external bias.

In figure 1.6 we show the $I - V$ characteristics when we include charging effects. We can clearly see that, instead of a sharp jump in the current once the bias exceeds $\frac{4}{e}|\epsilon_0 - \mu_0|$, the linear dependence of the on-site potential on the occupation leads to a linear $I - V$ characteristics, persisting until the maximum current for that particular state has been reached.

We can understand such behaviour using a very simple pictorial description. Let us assume for the sake of simplicity that initially our energy level is higher than the chemical potential μ_0 . Within the bias gap, the molecular state remains essentially

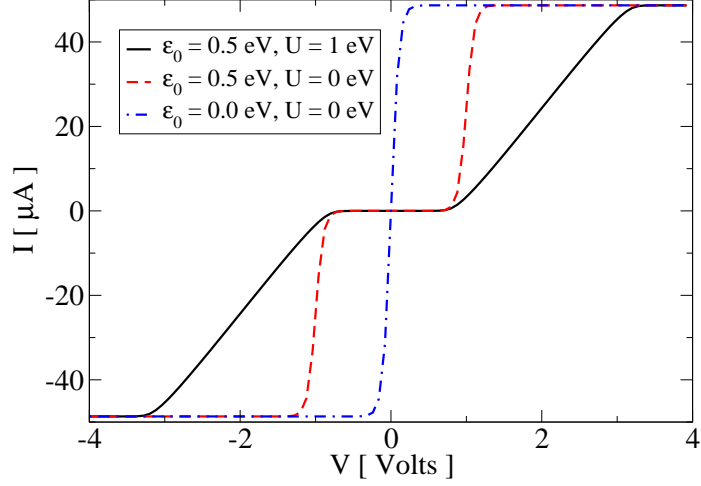


Figure 1.6: Current as a function of voltage for a molecule - represented by a single energy level - sandwiched between two electrodes. In this case $\Gamma_L = \Gamma_R = 1$ eV and the molecular energy level is positioned either at the initial chemical potential μ_0 (dashed-dotted line) or above it (solid). The on-site energy is set to 0 and 0.5 eV respectively and $U = 1$ eV. For comparison we also show the curve presented in figure (1.5) with $U = 0$ eV. Note that for $\epsilon = \mu_0 = 0$ eV charging has no effect in the $I - V$.

unchanged since there are no electrons providing additional charge. However when the energy level lies within the bias window it will start to charge, *i.e.*, its occupation which was originally zero will change. Once this happens the potential (equation (1.25)) shifts up accordingly to compensate for such an effect, and consequently the current drops because the position of that energy level is never completely within the bias window. The linear behaviour is essentially given by the linear dependence of the self-consistent potential on the occupation. When the bias is equal to $2|\mu_0 - \epsilon_0| + 2U$ (the factor 2 comes from the fact that we shift one electrode by $V/2$ and the other by $-V/2$), the potential cannot shift any higher and the current will reach its maximum value. As we mentioned earlier the maximum for the current is only given by the coupling to the electrodes Γ_L and Γ_R .

1.3.2 Asymmetries

If we analyse equation (1.23) in the case of no-charging effects ($\epsilon = \epsilon_0$), we will see that no matter what the coupling terms Γ_L and Γ_R are, the current will always be symmetric with respect to the applied bias. In fact, interchanging $\Gamma_L \rightleftharpoons \Gamma_R$ leaves the total current and the occupation unchanged.

In order to introduce asymmetries in the $I - V$ characteristics we must take

into consideration effects due to changes in the electron occupation in addition to different coupling strengths. Once that is done we can see that although the pre-factor in equation (1.23) remains the same, term

$$f(\epsilon, \mu_L) - f(\epsilon, \mu_R) \quad (1.27)$$

containing the Fermi functions now depends on the position of the molecular energy level ϵ . As discussed before, this energy level must be calculated self-consistently in the case of charging effects.

By expanding equation (1.25) using equations (1.26) and (1.22) we obtain

$$\epsilon = \epsilon_0 + U \left(\frac{\Gamma_L f(\epsilon, \mu_L) + \Gamma_R f(\epsilon, \mu_R)}{\Gamma_L + \Gamma_R} - 2f(\epsilon_0, \mu) \right). \quad (1.28)$$

Hence, with the introduction of charging effects we can clearly see that the position of the energy level ϵ is not invariant by interchanging $\Gamma_L \rightleftharpoons \Gamma_R$. Consequently asymmetries in the $I - V$ will arise due to both charging and asymmetric coupling.

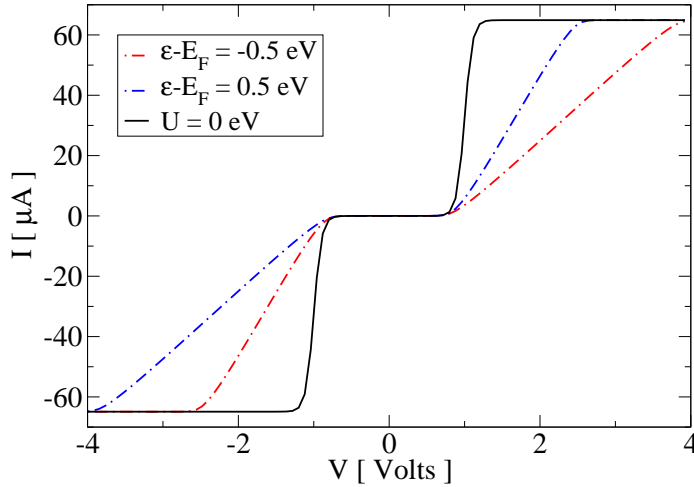


Figure 1.7: Current as a function of voltage for a molecule - represented by a single energy level - within two electrodes. In this case $\Gamma_L \neq \Gamma_R$ and the molecular energy level is positioned either at the Fermi level (solid curve), above (dashed) and below (dotted) the Fermi level. The on-site energy is set to 0, 1 and -1 eV respectively and we have included the effects of charging following equations (1.26) and (1.25) with $U = 1$ eV.

In figure (1.7) we show the effects of asymmetric coupling on the current either considering or not charging effects. We can clearly see that charging of the molecular level induces an asymmetric $I - V$ characteristics. This behaviour depends on the position of the molecular state ϵ_0 as well as the coupling constants.

Although over-simplified, this model brings into light a number of interesting aspects in electronic transport through molecular systems. We have shown that charging effects might have considerable implications for transport, more specifically, the combination of asymmetric coupling to the electrodes and charging leads to asymmetric current/voltage curves. A more realistic description of our system might eventually lead to rectification, an important mechanism in modern electronics.

Obviously, this model cannot account for realistic systems. In order to model material-dependent devices one must be able of describing the electronic properties of such systems with a large degree of accuracy. Moreover, charging must be correctly described if we wish to propose novel devices for logic applications.

In the next section we extend the ideas developed so far introducing an atomistic description of both the electrodes and the molecule. The electronic structure and consequently all other parameters describing our device are calculated with *ab initio* techniques. Hence, our simple model becomes a specific case in a more general theoretical framework known as non-equilibrium Green function formalism [90, 61].

1.4 Non–Equilibrium Transport

1.4.1 Non-equilibrium Green functions (NEGF) for an open system

As pointed out in the introduction we are dealing with an infinite-dimensional non-periodic Hermitian problem. The problem can be written down in terms of the retarded Green’s function \mathcal{G}^R for the whole system by solving the Green function equation

$$[\epsilon^+ \mathcal{S} - \mathcal{H}] \mathcal{G}^R(E) = \mathcal{I}, \quad (1.29)$$

where \mathcal{I} is an infinitely-dimensional identity matrix, $\epsilon^+ = \lim_{\delta \rightarrow 0^+} E + i\delta$ and E is the energy. The same equation explicitly using the block-diagonal structure of both the Hamiltonian and the overlap matrix (we drop the symbol “R” indicating the retarded quantities) is of the form

$$\begin{pmatrix} \epsilon^+ \mathcal{S}_L - \mathcal{H}_L & \epsilon^+ \mathcal{S}_{LM} - \mathcal{H}_{LM} & 0 \\ \epsilon^+ \mathcal{S}_{ML} - \mathcal{H}_{ML} & \epsilon^+ \mathcal{S}_M - \mathcal{H}_M & \epsilon^+ \mathcal{S}_{MR} - \mathcal{H}_{MR} \\ 0 & \epsilon^+ \mathcal{S}_{RM} - \mathcal{H}_{RM} & \epsilon^+ \mathcal{S}_R - \mathcal{H}_R \end{pmatrix} \begin{pmatrix} \mathcal{G}_L & \mathcal{G}_{LM} & \mathcal{G}_{LR} \\ \mathcal{G}_{ML} & \mathcal{G}_M & \mathcal{G}_{MR} \\ \mathcal{G}_{RL} & \mathcal{G}_{RM} & \mathcal{G}_R \end{pmatrix} = \begin{pmatrix} \mathcal{I} & 0 & 0 \\ 0 & I_M & 0 \\ 0 & 0 & \mathcal{I} \end{pmatrix}, \quad (1.30)$$

where we have partitioned the Green's functions \mathcal{G} into the infinite blocks describing the left- and right-hand side leads \mathcal{G}_L and \mathcal{G}_R , those describing the interaction between the leads and extended molecule \mathcal{G}_{LM} , \mathcal{G}_{RM} , the direct scattering between the leads \mathcal{G}_{LR} , and the finite block describing the extended molecule G_M . We have also introduced the matrices \mathcal{H}_L , \mathcal{H}_R , \mathcal{H}_{LM} , \mathcal{H}_{RM} and their corresponding overlap matrix blocks, indicating respectively the left- and right-hand-side leads Hamiltonian and the coupling matrix between the leads and the extended molecule. H_M is an $M \times M$ matrix and I_M is the $M \times M$ unit matrix. The infinite matrices, \mathcal{H}_L and \mathcal{H}_R describe the leads and have the following block-diagonal form

$$\mathcal{H}_L = \begin{pmatrix} \ddots & \ddots & \ddots & \ddots & \vdots \\ 0 & H_{-1} & H_0 & H_1 & 0 \\ \dots & 0 & H_{-1} & H_0 & H_1 \\ \dots & \dots & 0 & H_{-1} & H_0 \end{pmatrix}, \quad (1.31)$$

with similar expressions for \mathcal{H}_R and the overlap \mathcal{S} matrix counterparts. In contrast the coupling matrices between the leads and the extended molecule are infinite-dimensional matrices whose elements are all zero except for a rectangular block coupling the last PL of the leads and the extended molecule. For example we have

$$\mathcal{H}_{LM} = \begin{pmatrix} \vdots \\ 0 \\ H_{LM} \end{pmatrix}. \quad (1.32)$$

The crucial step in solving equation (1.30) is to write down the corresponding equation for the Green's function involving the EM and surface PL's of the left and right leads and then evaluate the retarded Green function for the extended molecule G_M^R . This can be done by returning to our initial assumptions about the electrostatics of the problem (section (1.1)); the potential drop occurs entirely across the extended molecule and there are no changes to the electronic structure of the charge reservoirs arising from neither the coupling to the molecule nor through the external bias. Bearing that in mind we can focus solely on the scattering region and treat the effect of electrodes in terms of an effective interaction.

This can be achieved by eliminating the degrees of freedom of the electrodes one by one from deep into the leads all the way to the interface with the EM. Effectively, one can renormalise the total Hamiltonian using a procedure that can be shown to be exact [65]. The final expression for G_M^R has the form

$$G_M^R(E) = [\epsilon^+ S_M - H_M - \Sigma_L^R(E) - \Sigma_R^R(E)]^{-1}, \quad (1.33)$$

where we have introduced the retarded self-energies for the left- and right-hand side lead

$$\Sigma_L^R(E) = (\epsilon^+ S_{ML} - H_{ML}) G_L^{0R}(E) (\epsilon^+ S_{LM} - H_{LM}) \quad (1.34)$$

and

$$\Sigma_R^R(E) = (\epsilon^+ S_{MR} - H_{MR}) G_R^{0R}(E) (\epsilon^+ S_{RM} - H_{RM}). \quad (1.35)$$

Here G_L^{0R} and G_R^{0R} are the retarded *surface* Green function of the leads, i.e. the leads retarded Green functions evaluated at the PL neighbouring the extended molecule when this one is decoupled from the leads. Formally G_L^{0R} (G_R^{0R}) corresponds to the right lower (left higher) block of the retarded Green's function for the whole left-hand side (right-hand side) semi-infinite lead. These are simply

$$\mathcal{G}_L^{0R}(E) = [\epsilon^+ \mathcal{S}_L - \mathcal{H}_L]^{-1} \quad (1.36)$$

and

$$\mathcal{G}_R^{0R}(E) = [\epsilon^+ \mathcal{S}_R - \mathcal{H}_R]^{-1}. \quad (1.37)$$

Note that \mathcal{G}_L^{0R} (\mathcal{G}_R^{0R}) is not the same as \mathcal{G}_L^R (\mathcal{G}_R^R) defined in equation (1.30). In fact the former are the Green functions for the semi-infinite leads in isolation, while the latter are the same quantities for the leads attached to the scattering region. Importantly one does not need to solve equations (1.36) and (1.37) for calculating the leads surface Green functions and a closed form avoiding the inversion of infinite matrices can be provided [65]. We will return to this discussion in more detail in section (1.6.2).

Let us conclude this section with a few comments on the results obtained. The retarded Green's function G_M^R contains all the information about the electronic structure of the extended molecule attached to the leads. In its close form given by the equation (1.33) it is simply the retarded Green's function associated to the effective Hamiltonian matrix H_{eff}

$$H_{\text{eff}} = H_M + \Sigma_L^R(E) + \Sigma_R^R(E).^7 \quad (1.38)$$

Note that H_{eff} is not Hermitian since the self-energies are not Hermitian matrices. This means the total number of particles in the extended molecule is not conserved, as expected by the presence of the leads. Moreover, since G_M^R contains all the information about the electronic structure of the extended molecule in equilibrium with

⁷Note that this is a more general case of equation (1.13). In the one level problem we set $H_M = \epsilon_0$ and $\Sigma_{L/R} = \Delta + i\Gamma_{L/R}/2$, with $\Delta = 0$. The real part of the self-energies shift the on-site energy level while the Γ 's provide the level broadening.

the leads, it can be directly used for extracting the zero-bias conductance G of the system. In fact one can simply apply the Fisher-Lee [61, 94] relation and obtain

$$G = \frac{2e^2}{h} \sum_{\text{Tr}} [\Gamma_{\text{L}} G^{\text{R}\dagger}_{\text{M}} \Gamma_{\text{R}} G_{\text{M}}^{\text{R}}], \quad (1.39)$$

where

$$\Gamma_{\alpha}(E) = i[\Sigma_{\alpha}^{\text{R}}(E) - \Sigma_{\alpha}^{\text{R}}(E)^{\dagger}], \quad (1.40)$$

($\alpha=\text{L,R}$). In equation (1.39) all the quantities are evaluated at the Fermi energy E_{F} . Clearly $\text{Tr}[\Gamma_{\text{L}} G^{\text{R}\dagger}_{\text{M}} \Gamma_{\text{R}} G_{\text{M}}^{\text{R}}](E)$ is simply the energy dependent total transmission coefficient $T(E)$ of standard scattering theory [84].

Finally note that what we have elaborated so far is an alternative way of solving a scattering problem. In standard scattering theory, as discussed in section (1.2), one first computes the asymptotic current carrying states deep into the leads (scattering channels) and then evaluates the quantum mechanical probabilities for these channels to be reflected and transmitted through the extended molecule [84]. The details of the scattering region are often reduced to a matrix describing the effective coupling between the two surface PLs of the leads which can be solve using a Green function [65] or transfer matrix approach [92]. In contrast the use of (1.39) describes an alternative though equivalent approach, in which the leads are projected out to yield a reduced matrix describing an effective EM. The current through surface PL's perpendicular to the transport direction are the same,⁸ the two approaches are equivalent and there is no clear advantage in using either one or the other. However, when the Hamiltonian matrix of the scattering region H_{M} is not known *a priori*, then the NEGF method offers a simple way of setting up a self-consistent procedure.

1.4.2 Steady-state and self-consistent procedure

Consider now the case in which the matrix elements of the Hamiltonian of the system are not known explicitly, but only their functional dependence upon the charge density $n(\vec{r})$, $\mathcal{H} = \mathcal{H}[n]$, is known. This is the most common case in standard mean field electronic structure theory, such as DFT [77, 78]. If no external bias is applied to the device (linear response limit) the Hamiltonian of the system can be simply obtained from a standard equilibrium DFT calculation and the procedure described in the previous section can be used without any modification. However, when an external bias V is applied, the charge distribution on the extended molecule will differ from

⁸Some caution should be taken in selecting the plane for evaluating the conductance when the basis set is not complete as in the case of LAO basis sets. See for instance [95] and [96].

the one at equilibrium since both the net charge and the electrical polarisation are affected by the bias. This will determine a new electrostatic potential profile with different scattering properties.

These modifications will affect only the extended molecule, since our leads preserve local charge neutrality. This means that the charge density and therefore the Hamiltonian of the leads are not modified by the external bias applied. As discussed at the beginning the only effect of the external bias over the current/voltage electrodes is a rigid shift of the on-site energies. The Hamiltonian then takes the form

$$\mathcal{H} = \begin{pmatrix} \mathcal{H}_L + \mathcal{S}_L eV/2 & \mathcal{H}_{LM} & 0 \\ \mathcal{H}_{ML} & H_M & \mathcal{H}_{MR} \\ 0 & \mathcal{H}_{RM} & \mathcal{H}_R - \mathcal{S}_R eV/2 \end{pmatrix}, \quad (1.41)$$

Note that the coupling matrices between the leads and the extended molecule are also not modified by the external bias, since by construction the charge density in the surface planes of the extended molecule matches exactly that of the leads.

The Hamiltonian of the extended molecule

$$H_M = H_M[n] \quad (1.42)$$

depends on the density matrix, which is calculated using the lesser Green function [61, 62, 63, 64, 71, 89, 90]

$$D_M = \frac{1}{2\pi i} \int dE G_M^<(E), \quad (1.43)$$

so a procedure must be devised to compute this quantity.

In equilibrium, $G^<(E) = -2i \text{Im} [G^R(E)] f(E - \mu)$, so it is only necessary to consider the retarded Green function, given by equation (1.33). Out of equilibrium, however, the presence of the leads establishes a non-equilibrium population in the extended molecule and $G^<$ is no longer equal to $-2i \text{Im} [G^R] f(E - \mu)$. The non-equilibrium Green function formalism [61, 62, 63, 64, 89, 90] provides the correct expression (see appendix C in [71]):

$$G_M^<(E) = iG_M^R(E)[\Gamma_L f(E - \mu_L) + \Gamma_R f(E - \mu_R)]G_M^{R\dagger}(E) \quad (1.44)$$

where $\mu_{L/R} = \mu \pm eV/2$, $f(x)$ is the Fermi function for a given temperature T ,

$$\Sigma_{L/R} = \Sigma_{L/R}(E, V), \quad (1.45)$$

and

$$\Gamma_{L/R} = \Gamma_{L/R}(E, V). \quad (1.46)$$

Our main assumption about the leads is that the effect of the bias induces a rigid shift in the electronic structure, hence it is easy to see that

$$\Sigma_{\text{L/R}}(E, V) = \Sigma_{\text{L/R}}(E \mp eV/2, V = 0) \quad (1.47)$$

and consequently

$$\Gamma_{\text{L/R}}(E, V) = \Gamma_{\text{L/R}}(E \mp eV/2, V = 0). \quad (1.48)$$

In other words, we can calculate the self-energies and the Γ matrices for zero bias and apply a shift of $\mp \frac{V}{2}$ to the electronic structure to mimic the applied bias.⁹

Finally, $G_{\text{M}}^{\text{R}}(E)$ is given again by equation (1.33) where now we replace $\Sigma_{\text{L/R}}(E)$ with $\Sigma_{\text{L/R}} = \Sigma_{\text{L/R}}(E \pm eV/2)$.

The self consistent procedure is as follows. First a trial charge density

$$n^0(\vec{r}) = \langle \vec{r} | D_{\text{M}}^0 | \vec{r} \rangle \quad (1.49)$$

is used to compute H_{M} from equation (1.42). Then Γ_{L} , Γ_{R} and G_{M}^{R} are calculated from equations (1.47), (1.48), and (1.33). These quantities are used to compute G_{M}^{L} in equation (1.44), which is fed back into equation (1.43) to find a new density n^1 . This process is iterated until a self-consistent solution is achieved, which is when

$$\text{Max} ||D_{\text{M}}^j - D_{\text{M}}^{j+1}|| < \delta, \quad (1.50)$$

where $\delta \ll 1$ is a tolerance parameter.

Finally, the current I can be calculated using [97]

$$I = \frac{e}{h} \int dE \text{Tr}[\Gamma_{\text{L}} G_{\text{M}}^{\text{R}\dagger} \Gamma_{\text{R}} G_{\text{M}}^{\text{R}}] (f(E - \mu_{\text{L}}) - f(E - \mu_{\text{R}})) . \quad (1.51)$$

Note that the term $\text{Tr}[\Gamma_{\text{L}} G_{\text{M}}^{\text{R}\dagger} \Gamma_{\text{R}} G_{\text{M}}^{\text{R}}]$ is analogous to the conductance for the linear regime (Eq. (1.11)). Hence we can associate

$$T(E, V) = \text{Tr}[\Gamma_{\text{L}} G_{\text{M}}^{\text{R}\dagger} \Gamma_{\text{R}} G_{\text{M}}^{\text{R}}], \quad (1.52)$$

with the transmission coefficient, which in the more general non-equilibrium case is bias-dependent as well as energy-dependent. Koentopp and Burke have shown that the Landauer-Büttiker formula only holds in the case of interacting electrons in the

⁹We can see that this is indeed the case by taking the Hamiltonian of an infinite system H and applying a constant potential V . The resulting eigenvalue equation is $H + VS = ES$ which becomes $H = (E - V)S$. It is then clear that the eigenvectors for this problem are unchanged when compared to the zero bias case and the eigenvalues are shifted by a constant V (assuming that the potential has converged deep inside the electrodes and all we see is a constant bias). Subsequently the charge density n remains the same provided we shift the Fermi level (chemical potential) by V .

limit of zero bias when the exchange and correlation term in the Hamiltonian is local. In the case of non-local potentials a correction due to the response to the external electric field in the exchange-correlation potential must be added [98].

Let us conclude this section with a note on how to perform the integrals of equations (1.43) and (1.51). The one for the current is trivial since the two Fermi functions effectively cut the integration to give a narrow energy window between the chemical potentials of the leads. In addition the transmission coefficients, with the exception of some tunnelling situations, is usually a smooth function of the energy.

In contrast, the integration leading to the density matrix (1.43) is more difficult, since the integral is unbound and the Green function has poles over the real energy axis. This however can be drastically simplified by adding and subtracting the term $G_M^R \Gamma_R G_M^{R\dagger} f(E - \mu_L)$ to equation (1.44) to yield after some rearrangements

$$G_M^<(E) = i \left[G_M^R(E) (\Gamma_L + \Gamma_R) G_M^{R\dagger}(E) f(E - \mu_L) + G_M^R(E) \Gamma_R G_M^{R\dagger}(E) (f(E - \mu_R) - f(E - \mu_L)) \right]. \quad (1.53)$$

We can note that

$$\begin{aligned} \Gamma_L + \Gamma_R &= i \left[\Sigma_L^R - \Sigma_L^{R\dagger} + \Sigma_R^R - \Sigma_R^{R\dagger} \right] = \\ &= i \left[(-\epsilon S_M + H_M + \Sigma_L^R + \Sigma_R^R) - (-\epsilon S_M^\dagger + H_M^\dagger + \Sigma_L^{R\dagger} + \Sigma_R^{R\dagger}) \right] \\ &= i \left[(G_M^{R\dagger})^{-1} - (G_M^R)^{-1} \right]. \end{aligned} \quad (1.54)$$

Therefore, by substituting equation (1.54) into equation (1.53) we obtain

$$G_M^<(E) = - \left(G_M^R - G_M^{R\dagger} \right) f(E - \mu_L) + i G_M^R \Gamma_R G_M^{R\dagger} (f(E - \mu_R) - f(E - \mu_L)), \quad (1.55)$$

which in turn reduces to

$$G_M^<(E) = -2i \text{Im} [G_M^R] f(E - \mu_L) + i G_M^R \Gamma_R G_M^{R\dagger} (f(E - \mu_R) - f(E - \mu_L)).^{10} \quad (1.56)$$

Based on the new form of $G_M^<(E)$, it is now possible to rewrite the integral (1.43) as the sum of two contributions $D = D_{\text{eq}} + D_V$

$$D_{\text{eq}} = -\frac{1}{\pi} \int dE \text{Im} [G_M^R] f(E - \mu_L), \quad (1.57)$$

and

$$D_V = \frac{1}{2\pi} \int dE G_M^R \Gamma_R G_M^{R\dagger} [f(E - \mu_R) - f(E - \mu_L)]. \quad (1.58)$$

¹⁰Considering G_M^R to be a symmetric matrix.

D_{eq} can be interpreted as the density matrix at equilibrium, *i.e.* the one obtained when both the reservoirs have the same chemical potential μ_L , while D_V contains all the corrections due to the non-equilibrium conditions. Computationally, D_V is bound by the two Fermi functions of the leads, in similar fashion to the current I , and therefore one needs to perform the integration only in the energy range between the two chemical potentials (see figure (1.8a)). In contrast D_{eq} is unbound, but the integral can be performed in the complex plane using a standard contour integral technique [99], since G_M^R is both analytical [100] and smooth.¹¹ Despite being unbound, in the lower part of the energy axis the integral of equation (1.57) only requires the inclusion of all occupied states (those below the Fermi level) of the extended molecule and of the bands of the electrodes. At energies below a certain threshold, the integrand goes to zero quite quickly. Hence we can choose a finite value for the lower limit of integration ensuring all the available states below E_F are counted. The point denoted **EnergLowestBound** - a parameter of the calculation - in Fig. (1.8) indicates that limit.

The integration in all cases is performed using a Gaussian quadrature (Gauss-Legendre) method [101].

1.5 Spin polarised systems: Collinear versus non-collinear spins

The Green function method described in the previous section can be generalised to magnetic systems or to other systems where the spin degree of freedom has to be taken into consideration (open-shell systems). We consider two different cases. The first is when spin up (majority) and spin down (minority) electrons are completely decoupled from each other in the sense that there is no spin-flip. This is the case of collinear-spin systems and in transport theory is known as the “two-spin fluid” approximation [102]. In this situation, the Hamiltonian, overlap matrix and all other operators have the form

$$A = \left(\begin{array}{c|c} A^\uparrow & 0 \\ \hline 0 & A^\downarrow \end{array} \right), \quad (1.59)$$

where the A^σ block describes the spin σ sub-band.

¹¹In the same way, we could add and subtract a term $G_M^R \Gamma_L G_M^{R\dagger} f(E - \mu_R)$ to equation (1.43) and work through the algebra to obtain equations which are analogous to (1.57) and (1.58). In practice, numerical errors arise when calculating the Green function which might lead to slight differences in the density matrix calculated by these two methods. In order to minimise the effects of numerical errors we perform an average of the density matrices obtained in the two possible ways.

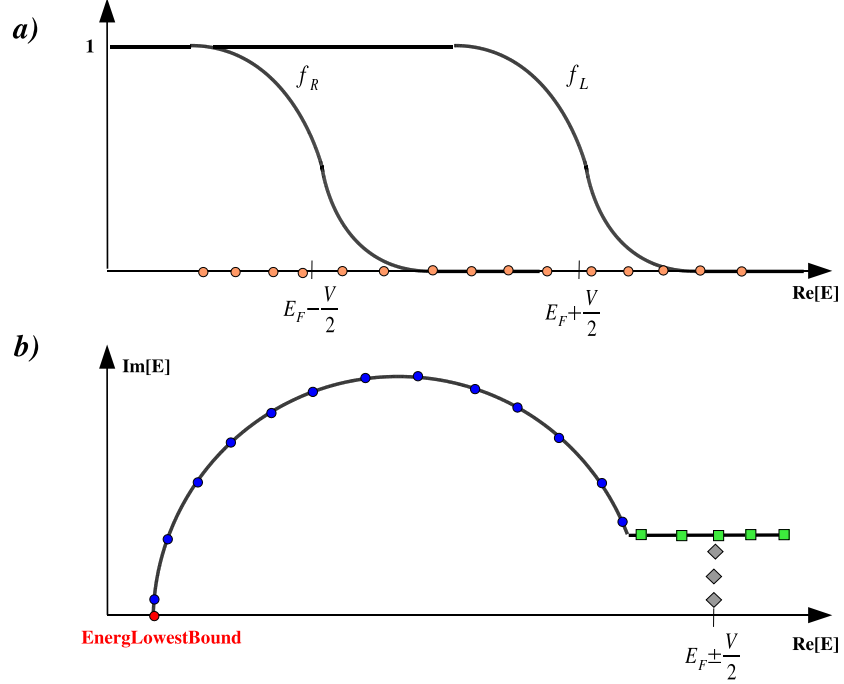


Figure 1.8: Diagram of the Green function integration leading to the non-equilibrium charge density. The non-equilibrium part must be performed along the real energy axis, but it is bound by the left- and right-hand side Fermi distribution functions, f_L and f_R . b) The integral for the equilibrium component is performed over a semicircular path in the complex energy plane. Here we show the lower limit of integration (below the lowest band of the electrodes), the energy mesh along the two segments of the curve and the poles of the Fermi distribution.

In this case we can work with two completely independent systems. Because majority and minority spins are effectively decoupled we can separate the two spins and calculate all quantities independently. The formalism described in section (1.4) still holds, but we need to introduce a new index which spans over the spin degree of freedom, σ . Operators such as the Hamiltonian, overlap matrix, Green function and density matrix are now written in the form

$$A_{ij}^{\sigma\sigma'} = A_{ij}^{\sigma\sigma'} \delta_{\sigma\sigma'} = A_{ij}^{\sigma} \quad (1.60)$$

Once convergence is achieved the total transmission and the total current are simply given by

$$T = \sum_{\sigma} T^{\sigma} = T^{\uparrow} + T^{\downarrow} \quad (1.61)$$

$$I = \sum_{\sigma} I^{\sigma} = I^{\uparrow} + I^{\downarrow}, \quad (1.62)$$

i. e., the contributions of the two spins add in parallel.

In the case we described above, the spins are always considered to be in an eigenstate of the spin operator S_z . We might want to consider cases where the magnetic moments are not aligned in the same way (non-collinear spins). In other words, we can envisage a situation where the magnetic moments of different atoms in our system are aligned at a certain angle with respect to each other. An example of such a system is presented in figure (1.9) where we show an array of atoms with a spiral-shaped magnetic moment. This is exactly the case in for example a domain wall [103, 104].

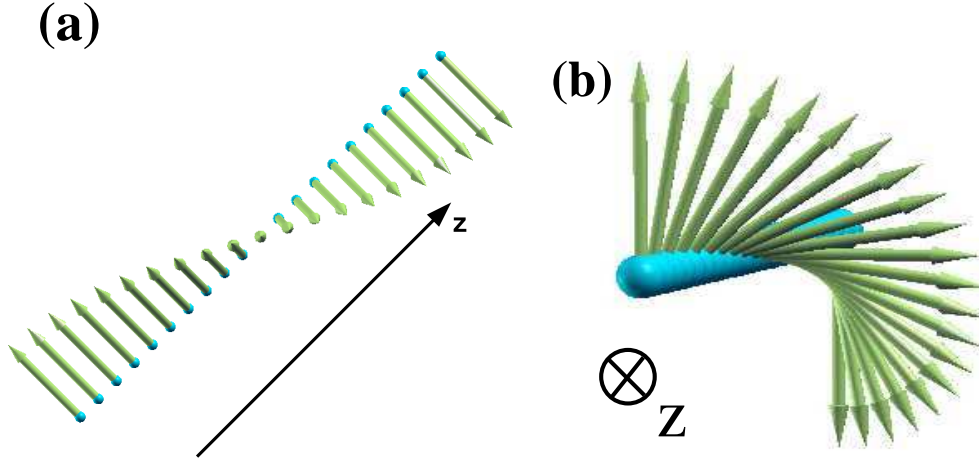


Figure 1.9: Infinite mono-atomic wire with arrows showing the direction of the magnetic moments for each atom. a) Diagonal and b) top views of the wire. Note that the magnitude of the spins are kept constant, but the magnetic moments are allowed to point in different directions.

In this case our operators have the following form ¹²

$$A = \left(\begin{array}{c|c} A^{\uparrow\uparrow} & A^{\uparrow\downarrow} \\ \hline A^{\downarrow\uparrow} & A^{\downarrow\downarrow} \end{array} \right) \quad (1.63)$$

The off-diagonal terms couple the up and down spins and are related to the angles between the magnetic moments.

Now, instead of working with different spins we use the NEGF formalism for a general spin direction. The total Hamiltonian has dimensions $2N \times 2N$. We can then define the Green function for this system in the form of equation (1.63),

$$G = \left(\begin{array}{c|c} G^{\uparrow\uparrow} & G^{\uparrow\downarrow} \\ \hline G^{\downarrow\uparrow} & G^{\downarrow\downarrow} \end{array} \right), \quad (1.64)$$

¹²Except for the overlap matrix which still retains the form of equation (1.59).

where

$$G^{\uparrow\uparrow} = \begin{pmatrix} ES_L^\uparrow - H_L^{\uparrow\uparrow} - \Sigma_L^{\uparrow\uparrow} & ES_{LM}^\uparrow - H_{LM}^{\uparrow\uparrow} & 0 \\ ES_{ML}^\uparrow - H_{ML}^{\uparrow\uparrow} & ES_M^\uparrow - H_M^{\uparrow\uparrow} & ES_{MR}^\uparrow - H_{MR}^{\uparrow\uparrow} \\ 0 & ES_{RM}^\uparrow - H_{RM}^{\uparrow\uparrow} & ES_R^\uparrow - H_R^{\uparrow\uparrow} - \Sigma_R^{\uparrow\uparrow} \end{pmatrix}, \quad (1.65)$$

$$G^{\uparrow\downarrow} = \begin{pmatrix} -H_L^{\uparrow\downarrow} - \Sigma_L^{\uparrow\downarrow} & -H_{LM}^{\uparrow\downarrow} & 0 \\ -H_{ML}^{\uparrow\downarrow} & -H_M^{\uparrow\downarrow} & -H_{MR}^{\uparrow\downarrow} \\ 0 & -H_{RM}^{\uparrow\downarrow} & -H_R^{\uparrow\downarrow} - \Sigma_R^{\uparrow\downarrow} \end{pmatrix}, \quad (1.66)$$

$$G^{\downarrow\uparrow} = \begin{pmatrix} -H_L^{\downarrow\uparrow} - \Sigma_L^{\downarrow\uparrow} & -H_{LM}^{\downarrow\uparrow} & 0 \\ -H_{ML}^{\downarrow\uparrow} & -H_M^{\downarrow\uparrow} & -H_{MR}^{\downarrow\uparrow} \\ 0 & -H_{RM}^{\downarrow\uparrow} & -H_R^{\downarrow\uparrow} - \Sigma_R^{\downarrow\uparrow} \end{pmatrix}, \quad (1.67)$$

$$G^{\downarrow\downarrow} = \begin{pmatrix} ES_L^\downarrow - H_L^{\downarrow\downarrow} - \Sigma_L^{\downarrow\downarrow} & ES_{LM}^\downarrow - H_{LM}^{\downarrow\downarrow} & 0 \\ ES_{ML}^\downarrow - H_{ML}^{\downarrow\downarrow} & ES_M^\downarrow - H_M^{\downarrow\downarrow} & ES_{MR}^\downarrow - H_{MR}^{\downarrow\downarrow} \\ 0 & ES_{RM}^\downarrow - H_{RM}^{\downarrow\downarrow} & ES_R^\downarrow - H_R^{\downarrow\downarrow} - \Sigma_R^{\downarrow\downarrow} \end{pmatrix}. \quad (1.68)$$

By using the Green function defined in equation (1.64) we can apply equations (1.57) and (1.58) as we did in section (1.4) after redefining the self-energies as

$$\Sigma_L = \left(\begin{array}{ccc|ccc} \Sigma_L^{\uparrow\uparrow} & 0 & 0 & \Sigma_L^{\uparrow\downarrow} & 0 & 0 \\ 0 & 0 & 0 & 0 & 0 & 0 \\ 0 & 0 & 0 & 0 & 0 & 0 \\ \hline \Sigma_L^{\downarrow\uparrow} & 0 & 0 & \Sigma_L^{\downarrow\downarrow} & 0 & 0 \\ 0 & 0 & 0 & 0 & 0 & 0 \\ 0 & 0 & 0 & 0 & 0 & 0 \end{array} \right), \quad (1.69)$$

and

$$\Sigma_R = \left(\begin{array}{ccc|ccc} 0 & 0 & 0 & 0 & 0 & 0 \\ 0 & 0 & 0 & 0 & 0 & 0 \\ 0 & 0 & \Sigma_R^{\uparrow\uparrow} & 0 & 0 & \Sigma_R^{\uparrow\downarrow} \\ \hline 0 & 0 & 0 & 0 & 0 & 0 \\ 0 & 0 & 0 & 0 & 0 & 0 \\ 0 & 0 & \Sigma_R^{\downarrow\uparrow} & 0 & 0 & \Sigma_R^{\downarrow\downarrow} \end{array} \right). \quad (1.70)$$

Γ_L and Γ_R can be calculated in an analogous way.

Finally, the density matrix (equation (1.43)) and the current (Eq. (1.51)) can be calculated using the procedure described previously.

Finally, let us conclude this section with a note on the Spin-Orbit (SO) interaction. Spin-Orbit coupling is a relativistic correction to the Schrödinger equation [105, 106] which increases with atomic number. While for materials formed from light atoms such an effect is negligible, for heavier atoms it plays an increasingly important role. In the case of 3d transition metals for example it is the cause of magnetic

anisotropies [107] of the order of 10-100 μeV and in semiconductors it causes the edges of the valence and the conduction band to spin-split [108].

When we consider the SO effect the spin is no longer a good quantum number. In turn one needs to consider the total angular momentum \vec{J} ($\vec{J} = \vec{S} + \vec{L}$: the sum of spin and orbital angular momenta). In essence, the SO coupling leads to off-diagonal terms in the Hamiltonian in similar fashion to Eq. (1.63). Therefore, the formalism described so far can be naturally extended to include SO effects in the transport properties of nanostructures provided we can write a Hamiltonian for the scattering region [109].

Hence, we have shown that the NEGF method can be generalised to include periodic boundary conditions in the transverse direction. This is particularly useful when dealing with transport through surfaces and hetero-junctions.

1.6 Leads' self-energies

1.6.1 Surface Green's functions

Let us now return to the question of how to calculate the self-energies for the leads. From equations (1.34) and (1.35) it is clear that the problem is reduced to that of computing the retarded surface Green functions for the left- (G_L^{OR}) and right-hand side (G_R^{OR}) lead respectively. This does not require any self-consistent procedure since the Hamiltonian is known and it is equal to that of the bulk leads plus a rigid shift of the on-site energies. However the calculation should be repeated several times since the Σ 's are energy dependent. Therefore it is crucial to have a stable algorithm.

There are a number of techniques in the literature to calculate the surface Green functions of a semi-infinite system. These range from recursive methods [61, 110] to semi-analytical constructions [65]. Here we have generalised the scheme introduced by Sanvito *et. al.* [65] to non-orthogonal basis sets. This method gives us a prescription for calculating the retarded surface Green function exactly. The main idea is to construct the Green function for an infinite system as a summation of Bloch states with both real and imaginary wave-vectors, and then to apply the appropriate boundary conditions to obtain the Green function for a semi-infinite lead.

As explained in section (1.1) the Hamiltonian and the overlap matrices are arranged in a tridiagonal block form, having respectively H_0 and S_0 on the diagonal, and H_1 and S_1 as the first off diagonal blocks (see figure 1.10)). Since we are dealing with an infinite periodic quasi-one-dimensional system, the Schrödinger equation can

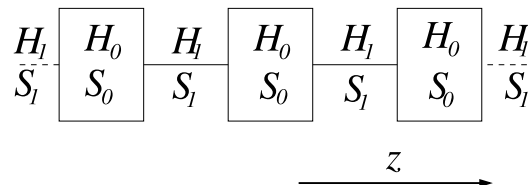


Figure 1.10: Infinite periodic system used as current/voltage probe and schematic diagram of the Hamiltonian. H_0 and S_0 are the matrices describing the Hamiltonian and the overlap within a PL, while H_1 and S_1 are the same quantities calculated between two adjacent PLs. The arrow indicates the direction of transport (here along the z axis).

be solved for Bloch states

$$\psi_z = n_k^{1/2} e^{ikz} \phi_k \quad (1.71)$$

and reads

$$\left[K_0 + K_1 e^{ik} + K_{-1} e^{-ik} \right] \phi_k = 0 \, , \quad (1.72)$$

where $z = a_0 j$ with j integer and a_0 the separation between principal layers, k is the wave-vector along the direction of transport (in units of π/a_0), ϕ_k is a N -dimensional column vector and n_k a normalisation factor. Here we introduce the $N \times N$ matrices

$$K_0 = H_0 - ES_0, \quad (1.73)$$

$$K_1 = H_1 - ES_1, \quad (1.74)$$

$$K_{-1} = H_{-1} - ES_{-1} . \quad (1.75)$$

Since the Green's functions are constructed at a given energy our task is to compute $k(E)$ (both real and complex) instead of $E(k)$ as conventionally done in band theory. A numerically efficient method to solve the “inverse” secular equation $k = k(E)$ is to map it onto an equivalent eigenvalue problem. It is simple to demonstrate [65] that the eigenvalues of the following $2N \times 2N$ non-Hermitian matrix

$$M = \begin{pmatrix} -K_1^{-1}K_0 & -K_1^{-1}K_{-1} \\ I_N & 0 \end{pmatrix} \quad (1.76)$$

for a given energy E are $e^{ik(E)}$ and that the upper N components of the eigenvectors are the vectors ϕ_k . Clearly for the solution of this eigenvalue problem one needs to invert K_1 . However, since K_1 is determined by the details of the physical system, the choice of basis set and of principal layer may be singular or severely ill-conditioned. This problem often originates from the fact that a few states within a PL do not couple to states in the nearest-neighbouring PLs, but it can also be due to the symmetry

of the problem. For example in the case of *ab initio* derived matrices this becomes unavoidable when one considers transition metals, where the strongly localised d shells coexist with rather delocalised s electrons. A possible solution to this problem is to consider an equivalent *generalised* eigenvalue problem, which does not require matrix inversion. However this solution is not satisfactory for two reasons. First the matrices still remain ill-conditioned and the general algorithm is rather unstable. Secondly for extreme cases we have discovered that the generalised eigenvalue solver cannot return meaningful eigenvalues (divisions by zero are encountered when dealing with some “critical” closed-channel, k imaginary). We therefore decide to use an alternative approach constructing a regularisation procedure for eliminating the singularities of K_1 . This must be performed before starting the actual calculation of the Green functions. We will return on this aspect in section 1.6.2. For the moment we assume that K_1 has been regularised and it is neither singular nor ill-conditioned.

When using orthogonal basis sets the knowledge of k and $\{\phi_k\}$ is sufficient to construct the retarded Green function for the doubly-infinite system, which has the form [65]

$$G_{zz'} = \begin{cases} \sum_l^N \phi_{k_l} e^{ik_l(z-z')} \tilde{\phi}_{k_l}^\dagger V^{-1} & z \geq z' \\ \sum_l^N \phi_{\bar{k}_l} e^{i\bar{k}_l(z-z')} \tilde{\phi}_{\bar{k}_l}^\dagger V^{-1} & z \leq z' \end{cases}, \quad (1.77)$$

where the summation runs over both real and imaginary k_l . In equation (1.77) k_l (\bar{k}_l) are chosen to be the right-moving or right-decaying (left-moving or left-decaying) Bloch states, i.e. those with either positive group velocity or having k -vector with positive imaginary part (negative group velocity or negative imaginary part). $\{\phi_{k_l}\}$ are the corresponding vectors, and V is defined in reference [65]. Finally $\{\tilde{\phi}_{k_l}\}$ is just the dual of $\{\phi_{k_l}\}$ obtained from

$$\tilde{\phi}_{k_l}^\dagger \phi_{k_m} = \delta_{lm} \quad (1.78)$$

$$\tilde{\phi}_{\bar{k}_l}^\dagger \phi_{\bar{k}_m} = \delta_{lm} \quad (1.79)$$

$$(1.80)$$

In the case of a non-orthogonal basis set the same expression is still valid if V is now defined as follows

$$V = \sum_l^N \left(H_1^\dagger - E S_1^\dagger \right) \left[\phi_{k_l} e^{-ik_l} \phi_{k_l}^\dagger - \phi_{\bar{k}_l} e^{-i\bar{k}_l} \phi_{\bar{k}_l}^\dagger \right]. \quad (1.81)$$

Finally the surface Green functions for a semi-infinite system can be obtained from those of the doubly-infinite one by an appropriate choice of boundary conditions.

For instance if we subtract the term

$$\Delta_z(z' - z_0) = \sum_{l,h}^N \phi_{\bar{k}_h} e^{i\bar{k}_h(z-z_0)} \phi_{\bar{k}_h}^\dagger \phi_{k_l} e^{ik_l(z_0-z')} \phi_{k_l}^\dagger V^{-1}, \quad (1.82)$$

from $G_{zz'}$ of equation (1.77) we obtain a new retarded Green function vanishing at $z = z_0$. Note that $\Delta_z(z' - z_0)$ is a linear combination of eigenvectors (wavefunctions) and therefore does not alter the causality of G .

In this way we obtain the final expression for the retarded surface Green functions of both the left- and right-hand side lead

$$G_L^0 = \left[I_N - \sum_{l,h} \phi_{\bar{k}_h} e^{-i\bar{k}_h} \phi_{\bar{k}_h}^\dagger \phi_{k_l} e^{ik_l} \phi_{k_l}^\dagger \right] V^{-1}, \quad (1.83)$$

$$G_R^0 = \left[I_N - \sum_{l,h} \phi_{k_h} e^{ik_h} \phi_{k_h}^\dagger \phi_{\bar{k}_l} e^{-i\bar{k}_l} \phi_{\bar{k}_l}^\dagger \right] V^{-1}. \quad (1.84)$$

Once these operators have been calculated it is easy to obtain the self-energies from equations (1.34) and (1.35). These need to be computed at the beginning of the calculation only for a given energy mesh.

1.6.2 The “ K_1 problem”

The method presented in section (1.6.1) to calculate the leads Green’s functions depends crucially on the fact that the coupling matrix between principal layers $K_1 = H_1 - ES_1$ is invertible and not ill-defined. However this is not necessarily the case since singularities can be present in K_1 as the result of poor coupling between PLs or because of symmetry reasons. Note also that since $K_1 = H_1 - ES_1$ the rank of K_1 may also depend on the energy E .

We now give a few examples illustrating how these singularities arise. Let us consider for the sake of simplicity an orthogonal nearest neighbour tight-binding model with only one s -like basis function per atom. In this case $K_1 = H_1$ is independent of energy. In figure (1.11) we present four possible cases for which H_1 is singular, by no means the only ones. In the picture the dots represent the atomic position, the lines the bonds and the dashed boxes enclose a PL. All the bonds are assumed to have the same strength, thus all hopping integrals γ are identical.

In the first case (figure (1.11a)) the PL coincides with the primitive unit cell of the system and therefore it is the smallest principal layer that can be constructed. However since every second atom in the cell does not couple with its mirror in the

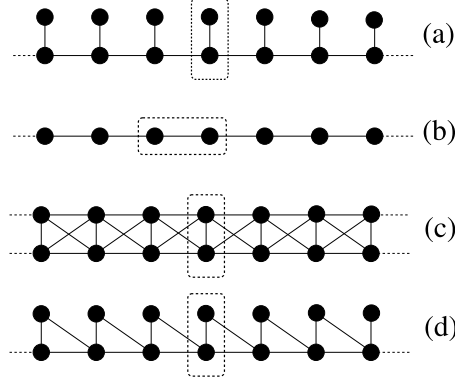


Figure 1.11: Four different structures for which H_1 is singular: (a) lack of bonding, (b) super-cell, (c) over-bonding, (d) odd bonding. Each black dot represents an atom and each line a bond. The dashed boxes enclose a principal layer.

two adjacent cells H_1 has the form

$$H_1 = \begin{pmatrix} \gamma & 0 \\ 0 & 0 \end{pmatrix} \quad (1.85)$$

and therefore is singular. This is the case of “lack of bonding” between principal layers. It is the most common case and almost always present when dealing with transition metals, since localised d shells coexist with delocalised s orbitals.

Figure (1.11b) presents a different possibility. Here the PL is a super-cell constructed from two unit cells and every atom in the PL couples with atoms located in only one of the two adjacent PLs. In this case

$$H_1 = \begin{pmatrix} 0 & 0 \\ \gamma & 0 \end{pmatrix}, \quad (1.86)$$

which is again singular. Clearly in this specific case one can reduce the principal layer into the primitive unit cell solving the problem (H_1 become a scalar γ). However in a multi-orbital scheme the super-cell drawn may be the smallest PL possible and the problem will appear. Again this is a rather typical situation when dealing with transition metals.

The case of “over-bonding” is shown in figure (1.11c). Again the PL coincides with the primitive unit cell, but now every atom in the PL is coupled to all the atoms in the two adjacent PLs. In this case

$$H_1 = \begin{pmatrix} \gamma & \gamma \\ \gamma & \gamma \end{pmatrix}, \quad (1.87)$$

which is not invertible either. This situation is usually driven by symmetry.

Finally the “odd-bonding” case is presented in figure (1.11d). Also in this case the PL coincides with the primitive unit cell, however the upper atom in the cell is coupled only to atoms in the right nearest neighbour principal layer. The H_1 matrix is then (we label as “1” the upper atom in the cell)

$$H_1 = \begin{pmatrix} 0 & \gamma \\ 0 & \gamma \end{pmatrix}, \quad (1.88)$$

i.e. it is also singular.

Clearly the above categorisation is basis dependent, since one can always find a unitary rotation transforming a generic H_1 in a new matrix of the form of equation (1.88).

1.6.3 Finding the singularities of K_1

We now present the first step of a scheme for regularising K_1 , and indeed the whole Hamiltonian and overlap matrix, by removing their singularities. In the cases of “lack of bonding”, “super-cell” and “odd-bonding” presented in the previous section the singularities of $K_1 = H_1$ were well defined since an entire column was zero. However more generally, and in particular in the case of multiple zetas basis set, K_1 is singular without having such a simple structure (for instance as in the “over-bonding” case). This is the most typical situation and a method for identifying the singularities is needed.

The ultimate goal is to perform a unitary transformation of both \mathcal{H} and \mathcal{S} in such a way that the off-diagonal blocks of the leads Hamiltonian and overlap matrix (H_1 and S_1) assume the form

$${}^N_{N-R} \begin{bmatrix} 0 & A \end{bmatrix} = \begin{pmatrix} 0 & 0 & \cdots & A_{1,N-R+1} & \cdots & A_{1,N} \\ 0 & 0 & \cdots & A_{2,N-R+1} & \cdots & A_{2,N} \\ 0 & 0 & \cdots & A_{3,N-R+1} & \cdots & A_{3,N} \\ \vdots & \vdots & \vdots & \vdots & \vdots & \vdots \\ 0 & 0 & \cdots & A_{N,N-R+1} & \cdots & A_{N,N} \end{pmatrix}, \quad (1.89)$$

i.e. they are $N \times N$ block matrices of rank R , whose first $N - R$ columns vanish. In this form the problem is re-conducted to the problem of “odd-bonding” presented in the previous section.

This can be achieved by performing a generalised singular value decomposition (GSVD) [111]. The idea is that a pair of $N \times N$ matrices, in this case H_1 and S_1 , can be written in the following form

$$H_1 = U \Lambda_1 [0, W] Q^\dagger, \quad (1.90)$$

$$S_1 = V \Lambda_2 [0, W] Q^\dagger, \quad (1.91)$$

plus extended molecule). These are given by $\mathcal{Q}^\dagger \mathcal{H} \mathcal{Q}$ and $\mathcal{Q}^\dagger \mathcal{S} \mathcal{Q}$ with the infinite matrix \mathcal{Q} defined as

$$\mathcal{Q} = \begin{pmatrix} \ddots & \cdot & \cdot & \cdot & \cdot & \cdot & \cdot & \cdot & \cdot \\ \cdot & 0 & Q & 0 & \cdot & \cdot & \cdot & \cdot & \cdot \\ \cdot & \cdot & 0 & Q & 0 & \cdot & \cdot & \cdot & \cdot \\ \cdot & \cdot & \cdot & 0 & I_M & 0 & \cdot & \cdot & \cdot \\ \cdot & \cdot & \cdot & \cdot & 0 & Q & 0 & \cdot & \cdot \\ \cdot & \cdot & \cdot & \cdot & \cdot & 0 & Q & 0 & \cdot \\ \cdot & \cdot & \cdot & \cdot & \cdot & \cdot & \cdot & \cdot & \ddots \end{pmatrix}, \quad (1.100)$$

where I_M is the $M \times M$ unit matrix. Note that this unitary transformation rotates all the H_1 matrices (the S_1 matrices in the case of \mathcal{S}), but leaves H_M (S_M) unchanged. Finally the matrices coupling the extended molecule to the leads transform as follows

$$\begin{aligned} H_{LM}^Q &\rightarrow Q^\dagger H_{LM}, \\ H_{ML}^Q &\rightarrow H_{ML} Q, \\ H_{RM}^Q &\rightarrow Q^\dagger H_{RM}, \\ H_{MR}^Q &\rightarrow H_{MR} Q, \end{aligned} \quad (1.101)$$

and so do the corresponding matrices of \mathcal{S} .

1.6.4 Solution of the “ K^1 problem”

Now that both \mathcal{H} and \mathcal{S} have been written in a convenient form we can efficiently renormalise them out. The key observation is that the two (infinite) blocks describing the leads have now the following structure (the \mathcal{S} matrix has an analogous structure and it is not shown here explicitly)

$$\begin{aligned} \mathcal{H}_{L/R}^Q &= \begin{pmatrix} \ddots & \vdots & \vdots & \vdots & \\ \cdots & Q^\dagger H_0 Q & Q^\dagger H_1 Q & 0 & \cdots \\ \cdots & Q^\dagger H_{-1} Q & Q^\dagger H_0 Q & Q^\dagger H_1 Q & \cdots \\ \cdots & 0 & Q^\dagger H_{-1} Q & Q^\dagger H_0 Q & \cdots \\ \vdots & \vdots & \vdots & \vdots & \ddots \end{pmatrix} = \\ &= \begin{pmatrix} \ddots & \vdots & \vdots & \vdots & \\ \cdots & Q^\dagger H_0 Q & \begin{bmatrix} 0 & \bar{H}_1 \end{bmatrix} & 0 & \cdots \\ \cdots & \begin{bmatrix} 0 \\ \bar{H}_1^\dagger \end{bmatrix} & \begin{pmatrix} C & B \\ B^\dagger & D \end{pmatrix} & \begin{bmatrix} 0 & \bar{H}_1 \end{bmatrix} & \cdots \\ \cdots & 0 & \begin{bmatrix} 0 \\ \bar{H}_1^\dagger \end{bmatrix} & \begin{pmatrix} C & B \\ B^\dagger & D \end{pmatrix} & \cdots \\ \vdots & \vdots & \vdots & \vdots & \ddots \end{pmatrix}, \end{aligned} \quad (1.102)$$

where the matrices D , B and C are respectively $R \times R$, $N \times (N - R)$ and $(N - R) \times (N - R)$.

Note that the degrees of freedom (orbitals) contained in the block C of the matrix $H_0^Q = Q^\dagger H_0 Q$ couple to those of only one of the two adjacent PLs. This situation is the generalisation to a multi-orbital non-orthogonal tight-binding model of the “odd bonding” case discussed at the beginning of this section (figure 1.11d). These degrees of freedom are somehow redundant and they will be eliminated. We therefore proceed with performing Gaussian elimination [65] (also known as “decimation”) of all the degrees of freedom associated to all the blocks C .

The idea is that the Schrödinger equation $Q^\dagger[\mathcal{H} - ES]Q\Psi = 0$ can be re-arranged in such a way that a subset of degrees of freedom (in this case those associated to orbitals in a PL that couple only to one adjacent PL) do not appear explicitly. The procedure is recursive. Let us suppose we wish to eliminate the l -th row and column of the matrix $\mathcal{K}^Q = Q^\dagger[\mathcal{H} - ES]Q$. This can be done by re-arranging the remaining matrix elements according to

$$\mathcal{K}_{ij}^{Q(1)} = \mathcal{K}_{ij}^Q - \frac{\mathcal{K}_{il}^Q \mathcal{K}_{lj}^Q}{\mathcal{K}_{ll}^Q}. \quad (1.103)$$

The dimension of the resulting new matrix $\mathcal{K}^{Q(1)}$ (“1” indicates that one decimation has been performed) is reduced by one with respect to the original \mathcal{K}^Q . This procedure is then repeated and after r decimations we obtain a matrix

$$\mathcal{K}_{ij}^{Q(r)} = \mathcal{K}_{ij}^{Q(r-1)} - \frac{\mathcal{K}_{il}^{Q(r-1)} \mathcal{K}_{lj}^{Q(r-1)}}{\mathcal{K}_{ll}^{Q(r-1)}}. \quad (1.104)$$

Let us now decimate all the matrix elements contained in all the sub-matrices C . We obtain a new tridiagonal matrix $\mathcal{K}^{Q(\infty)}$ (“ ∞ ” means that an infinite number of decimations have been performed) of the form

$$\mathcal{K}^{Q(\infty)} = \begin{pmatrix} \cdot & \cdot & \cdot & \cdot & \cdot & \cdot & \cdot & \cdot & \cdot & \cdot & \cdot \\ 0 & \Theta^\dagger & \Delta & \Theta & 0 & \cdot & \cdot & \cdot & \cdot & \cdot & \cdot \\ \cdot & 0 & \Theta^\dagger & \Delta & T_1 & 0 & \cdot & \cdot & \cdot & \cdot & \cdot \\ \cdot & \cdot & 0 & T_1^\dagger & D_1 & K_{\text{LM}}^Q & 0 & \cdot & \cdot & \cdot & \cdot \\ \cdot & \cdot & \cdot & 0 & K_{\text{ML}}^Q & K_{\text{M}} & \Theta_{\text{MR}} & 0 & \cdot & \cdot & \cdot \\ \cdot & \cdot & \cdot & \cdot & 0 & \Theta_{\text{RM}} & D_2 & \Theta & 0 & \cdot & \cdot \\ \cdot & \cdot & \cdot & \cdot & \cdot & 0 & \Theta^\dagger & \Delta & \Theta & 0 & \cdot \\ \cdot & \cdot & \cdot & \cdot & \cdot & \cdot & 0 & \Theta^\dagger & \Delta & \Theta & 0 \\ \cdot & \cdot & \cdot & \cdot & \cdot & \cdot & \cdot & \cdot & \cdot & \cdot & \cdot \end{pmatrix}, \quad (1.105)$$

where $K_{\text{LM}}^Q = H_{\text{LM}}^Q - ES_{\text{LM}}^Q$, $K_{\text{ML}}^Q = H_{\text{ML}}^Q - ES_{\text{ML}}^Q$ and $K_{\text{M}} = H_{\text{M}} - ES_{\text{M}}$. The crucial point is that the new matrix $\mathcal{K}^{Q(\infty)}$ is still in the desired tridiagonal form, but now

the coupling matrices between principal layers Θ are not singular. These are now $R \times R$ matrices obtained from the decimation of the non-coupled degrees of freedom of the matrices K_1^Q . Moreover the elimination of degrees of freedom achieved with the decimation scheme is carried out only in the leads. The electronic structure of these is not updated during the self-consistent procedure for evaluating the Green's function, and therefore the information regarding the decimated degrees of freedom are not necessary. In contrast the degrees of freedom of the scattering region are not affected by the decimation or the rotation. Therefore the matrix K_M is unaffected by the decimation.

In the decimated matrix $\mathcal{K}^{Q(\infty)}$ new terms appear (D_1, D_2, T_1 and Θ_{MR}). These arise from the specific structure of the starting matrix $\mathcal{Q}^\dagger[\mathcal{H} - E\mathcal{S}]\mathcal{Q}$ and from the fact that the complete system (leads plus scattering region) is not periodic. In fact assuming that j is the last principal layer of the left-hand side lead and l is the first layer of right-hand side lead, the decimation is carried out up to $j - 1$ to the left and starts from l to the right of the scattering region. This allows us to preserve the tridiagonal form of \mathcal{K} and at the same time to leave K_M unchanged. A schematic picture of the decimation strategy is illustrated in figure 1.12.

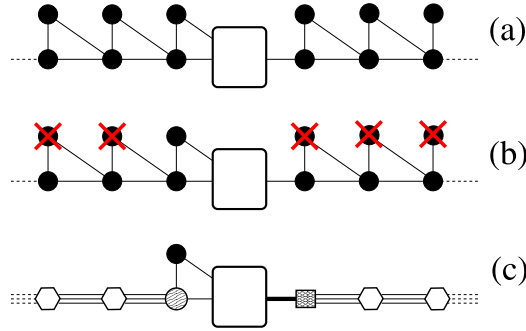


Figure 1.12: Schematic representation of the decimation strategy for the rotated \mathcal{K} matrix. Every symbol (dots, boxes ..) represents a collection of degrees of freedom (a matrix block) and every line the coupling. (a) Original structure after the rotation \mathcal{Q} . In the periodic leads the upper black dots represent the blocks C of the matrix of equation (1.6.4). The large white rectangular box represents the scattering region. (b) The degrees of freedom marked with the red crosses are decimated. (c) Final structure after decimation. The new white symbols represent the leads degrees of freedom of the principal layers adjacent to the scattering region as they appear after the decimation.

In practical terms all the blocks of the infinite matrix of equation (1.105) can be calculated by decimating auxiliary finite matrices. In particular

1. Δ , Θ and D_2 are calculated by decimating both the C matrices of the following finite $2N \times 2N$ matrix

$$\left(\begin{pmatrix} C & B \\ B^\dagger & D \end{pmatrix} \quad \begin{bmatrix} 0 & \bar{K}_1 \end{bmatrix} \right) \longrightarrow \begin{pmatrix} D_2 & \Theta \\ \Theta^\dagger & \Delta \end{pmatrix}, \quad (1.106)$$

where $\bar{K}_1 = \bar{H}_1 - E\bar{S}_1$ and

$$\begin{pmatrix} C & B \\ B^\dagger & D \end{pmatrix} = H_0^Q - ES_0^Q. \quad (1.107)$$

2. D_1 and T_1 are calculated by decimating only the upper C matrix of the same finite $2N \times 2N$ matrix

$$\left(\begin{pmatrix} C & B \\ B^\dagger & D \end{pmatrix} \quad \begin{bmatrix} 0 & \bar{K}_1 \end{bmatrix} \right) \longrightarrow \begin{pmatrix} D_2 & T_1 \\ T_1^\dagger & D_1 \end{pmatrix}, \quad (1.108)$$

where D_1 is $N \times N$, while T_1 is $R \times N$.

3. Θ_{MR} is a $M \times R$ matrix obtained by decimating the C block of the following $(N + M) \times (N + M)$ matrix

$$\left(\begin{matrix} 0_M & K_{\text{MR}}^Q \\ K_{\text{RM}}^Q & \begin{pmatrix} C & B \\ B^\dagger & D \end{pmatrix} \end{matrix} \right) \longrightarrow \begin{pmatrix} 0_M & \Theta_{\text{MR}} \\ \Theta_{\text{RM}} & D_2 \end{pmatrix}, \quad (1.109)$$

where 0_M is the M -dimensional null matrix.

Finally we are now in the position for calculating the self-energies. These are obtained from the surface Green's functions for the rotated and decimated leads (specified by the matrices Δ and Θ) and have the following form

$$\Sigma_L = K_{\text{ML}}^Q \left(-D_1 - T_1^\dagger G_L T_1 \right)^{-1} K_{\text{LM}}^Q \quad (1.110)$$

and

$$\Sigma_R = \Theta_{\text{MR}} \left[G_{\text{R}}^{-1} - (D_2 - \Delta) \right]^{-1} \Theta_{\text{RM}}. \quad (1.111)$$

Clearly our procedure not only regularises the algorithm for calculating the self-energies, giving it the necessary numerical stability, but also drastically reduces the degrees of freedom (orbitals) needed for solving the transport problem. These go

Finally it is important to note that usually the rank R of $\begin{bmatrix} H_1 \\ S_1 \end{bmatrix}$ is not necessarily the same of that of $\begin{bmatrix} H_1^\dagger \\ S_1^\dagger \end{bmatrix}$ (R'). If $R' < R$ the GSVD transformation must be performed over the matrices H_1^\dagger and S_1^\dagger . The procedure is similar to what described before but the final structure of the matrix \mathcal{K} is somehow different, and so should be the decimation scheme.

$$H_1^\dagger = U \Lambda_1 [0, W] Q^\dagger, \quad (1.112)$$

$$\mathcal{H}_{\text{L/R}}^Q = \begin{pmatrix} \ddots & \vdots & \vdots & \vdots & \\ \cdots & Q^\dagger H_0 Q & Q^\dagger H_1 Q & 0 & \cdots \\ \cdots & Q^\dagger H_{-1} Q & Q^\dagger H_0 Q & Q^\dagger H_1 Q & \cdots \\ \cdots & 0 & Q^\dagger H_{-1} Q & Q^\dagger H_0 Q & \cdots \\ & \vdots & \vdots & \vdots & \ddots \end{pmatrix} = \quad (1.114)$$

$$\begin{pmatrix} \ddots & \vdots & \vdots & \vdots & \\ \cdots & Q^\dagger H_0 Q & \begin{bmatrix} 0 \\ \bar{H}_1 \end{bmatrix} & 0 & \cdots \\ \cdots & [0 \quad \bar{H}_1^\dagger] & \begin{pmatrix} C & B \\ B^\dagger & D \end{pmatrix} & \begin{bmatrix} 0 \\ \bar{H}_1 \end{bmatrix} & \cdots \\ \cdots & 0 & [0 \quad \bar{H}_1^\dagger] & \begin{pmatrix} C & B \\ B^\dagger & D \end{pmatrix} & \cdots \\ & \vdots & \vdots & \vdots & \ddots \end{pmatrix}, \quad (1.115)$$

$$\mathcal{K}^{\mathcal{Q}(\infty)} = \begin{pmatrix} \dot{0} & \dot{\Theta}^\dagger & \dot{\Delta} & \dot{\Theta} & \dot{0} & \dot{\cdot} & \dot{\cdot} & \dot{\cdot} & \dot{\cdot} & \dot{\cdot} & \dot{\cdot} \\ \dot{\cdot} & \dot{0} & \dot{\Theta}^\dagger & \dot{\Delta} & \dot{\Theta} & \dot{0} & \dot{\cdot} & \dot{\cdot} & \dot{\cdot} & \dot{\cdot} & \dot{\cdot} \\ \dot{\cdot} & \dot{\cdot} & \dot{0} & \dot{\Theta} & D_2 & \Theta_{\text{LM}} & 0 & \dot{\cdot} & \dot{\cdot} & \dot{\cdot} & \dot{\cdot} \\ \dot{\cdot} & \dot{\cdot} & \dot{\cdot} & \dot{0} & \Theta_{\text{ML}} & K_{\text{M}}^{\mathcal{Q}} & K_{\text{MR}}^{\mathcal{Q}} & 0 & \dot{\cdot} & \dot{\cdot} & \dot{\cdot} \\ \dot{\cdot} & \dot{\cdot} & \dot{\cdot} & \dot{\cdot} & 0 & K_{\text{RM}}^{\mathcal{Q}} & D_1 & T_1 & 0 & \dot{\cdot} & \dot{\cdot} \\ \dot{\cdot} & \dot{\cdot} & \dot{\cdot} & \dot{\cdot} & \dot{\cdot} & 0 & T_1^\dagger & \Delta & \Theta & 0 & \dot{\cdot} \\ \dot{\cdot} & \dot{\cdot} & \dot{\cdot} & \dot{\cdot} & \dot{\cdot} & \dot{\cdot} & 0 & \Theta^\dagger & \Delta & \Theta & 0 \end{pmatrix}, \quad (1.116)$$

Albeit, it is clear that the diagonal part of the leads' Hamiltonians have a slightly different structure, a similar decimation procedure can be done on the total Hamiltonian. The resulting \mathcal{K}^Q is written using matrices calculated in analogous form. In practice:

1. Δ , Θ and D_2 are calculated by decimating both the C matrices of the following finite $2N \times 2N$ matrix

$$\left(\begin{pmatrix} C & B \\ B^\dagger & D \end{pmatrix} \quad \begin{bmatrix} 0 \\ \bar{K}_1 \end{bmatrix} \right) \longrightarrow \begin{pmatrix} \Delta & \Theta \\ \Theta^\dagger & D_2 \end{pmatrix}, \quad (1.117)$$

where $\bar{K}_1 = \bar{H}_1 - E\bar{S}_1$ and

$$\begin{pmatrix} C & B \\ B^\dagger & D \end{pmatrix} = H_0^Q - ES_0^Q. \quad (1.118)$$

2. D_1 and T_1 are calculated by decimating only the lower C matrix of the same finite $2N \times 2N$ matrix

$$\left(\begin{pmatrix} C & B \\ B^\dagger & D \end{pmatrix} \quad \begin{bmatrix} 0 \\ \bar{K}_1 \end{bmatrix} \right) \longrightarrow \begin{pmatrix} D_1 & T_1 \\ T_1^\dagger & D_2 \end{pmatrix}, \quad (1.119)$$

where D_1 is $N \times N$, while T_1 is $R \times N$.

3. Θ_{ML} is a $M \times R$ matrix obtained by decimating the C block of the following $(N + M) \times (N + M)$ matrix

$$\left(\begin{pmatrix} C & B \\ B^\dagger & D \end{pmatrix} \quad \begin{matrix} K_{LM}^Q \\ 0_M \end{matrix} \right) \longrightarrow \begin{pmatrix} D_2 & \Theta_{LM} \\ \Theta_{ML} & 0_M \end{pmatrix}, \quad (1.120)$$

where 0_M is the M -dimensional null matrix.

It is easy to see that the self-energies for the system using this particular transformation are

$$\Sigma_L = \Theta_{ML} [G_L^{-1} - (D_2 - \Delta)]^{-1} \Theta_{LM}. \quad (1.121)$$

and

$$\Sigma_R = K_{MR}^Q \left(-D_1 - T_1^\dagger G_R T_1 \right)^{-1} K_{RM}^Q. \quad (1.122)$$

1.7 Conclusion

In this chapter we have presented a comprehensive description of the non-equilibrium Green function formalism applied to transport. We have shown how to describe the transport problem specially under the effects of an external applied bias. The Green function can be used to calculate the steady state charge density and a self-consistent procedure can be put in place provided the system's Hamiltonian is a functional of this charge density - or the density matrix.

We have also shown that it is not necessary to treat the entire open system, but on the contrary we can focus on the scattering region and add the effects of the electrodes in terms of self-energies which are only statically (non-self-consistently) affected by the external potential. These self-energies, specially in the case of localised d orbitals might be difficult to compute and singularities in the Hamiltonian usually arise. Using the generalised singular value decomposition (GSVD) with non-orthogonal basis sets we can pin point all the states which are uncoupled and an automatic regularisation procedure is used to remove such singularities. This final procedure is very robust and leads to the decimation of a large number of states which are not directly linked to the transport properties or the density matrix of the scattering region, but indirectly influence its calculation.

The procedure presented in this chapter is very general. In principle, one could use any Hamiltonian form to calculate the Green function. In the next chapter we will present an implementation of this method within density functional theory which provides a framework for calculating accurate electronic structures and hence precise electronic transport properties.

